

Transparency fluctuations in randomly inhomogeneous barriers of finite area

M. É. Raïkh and I. M. Ruzin

A. F. Ioffe Physicotechnical Institute, Academy of Sciences of the USSR

(Submitted 28 November 1986)

Zh. Eksp. Teor. Fiz. **92**, 2257–2276 (June 1987)

The transparency of a finite-area specimen acting as a tunneling barrier for electrons is considered. When the barrier parameters undergo spatial fluctuations, the specific transparency is determined by punctures, i.e., by infrequent, widely spaced regions whose transparencies are exponentially large relative to the typical transparency. Because the number of perforations and their transparency for a specimen of finite thickness are random variables, the specific transparency varies from one specimen to another. The distribution functions for the logarithm of the transparency are calculated for specimens of large, small, and intermediate area. When an external factor such as an applied electric field is varied, a distinctive type of mesoscopic effect arises in which the logarithm of the transparency oscillates over the width of the distribution function. The oscillations are characterized by the correlation function for the transparency logarithm, which is calculated for several external field strengths.

I. INTRODUCTION

We consider a flat specimen of finite area which acts as a tunneling barrier for electrons. The barrier parameters are assumed to fluctuate randomly in space due, e.g., to surface roughness or random fluctuations in the potential of impurities present in the barrier. Since the barrier transparency depends exponentially on its dimensions, even small fluctuations of the latter can cause the local transparency to vary exponentially. If the area of the barrier is large, the main contribution to the average transparency will come from perforation, i.e., from exponentially sparse regions in which the transparency is exponentially large compared to the typical value. To calculate the average transparency one must consider a perforation which is optimal, i.e., for which the transparency times the probability of formation is a maximum. Several special cases of this problem have been solved in Refs. 1–5.

Let us now suppose that the area of specimen is so small that the average number of optimal perforation over its area is less than 1. Clearly, in this case the specific transparency will fluctuate by up to $\sim 100\%$ from one specimen to the next, and its logarithm will thus fluctuate by an amount of the order of unity; in this case, only the distribution function of the specific transparency for a population of specimens is meaningful. This situation was first analyzed in Ref. 6, where wave transmission through a finite system of independent filaments containing randomly distributed impurities was studied. It was shown there that the maximum of the distribution function (DF) for the logarithm of the specific transparency is determined by the most transparent of the perforations (the number of such perforations per specimen is typically of order unity). The distribution function itself was not calculated.

In this paper we calculate the DF for the logarithm of the specific transparency for a population of specimens. We show that the DF differs qualitatively for specimens with large, small, and intermediate areas. For large areas the DF is gaussian with width inversely proportional to the square root of the area; the position of the maximum is determined by the optimal perforations and is independent of the area. For intermediate areas, the maximum of the DF corre-

sponds to the same transparency as in the large-area case, but the DF is not gaussian; its width is much less than unity and depends in a very complicated way on the area. Finally, for small areas the area-dependence of the DF maximum is described by the results in Ref. 6, while the width of the DF is ~ 1 and increases with decreasing area.

Let us now assume that the local transparency of the barrier varies exponentially in response to some external agent (e.g., due to a change in barrier shape caused by an applied electric field). The resulting change in the transparency of the perforations will then vary from one puncture to another, and hence so will their relative contributions to the specific transparency of the specimen. In addition, the number of perforations giving the dominant contribution to the specific transparency may also change. In this paper we analyze how the DF changes in response to an external agent and show that the effects are equivalent to those produced by varying the area of the specimen.

We will also show that changes in the external agent alter the properties of the perforations responsible for the characteristic deviation of the transparency logarithm for a given specimen from its average value over a population of specimens. The effect of changing the external agent is thus equivalent to changing the random configuration of the impurities in the specimen (or the random potential), i.e., to replacing one specimen by another. It should therefore be possible using a single specimen to observe a distinctive mesoscopic effect similar to the one studied in Refs. 7–9, in which the transparency logarithm was found to oscillate over the width of the DF as the external agent was varied. The oscillations are characterized quantitatively by the correlation functions of the transparency logarithm for various types of external agents. In this paper we calculate the correlation function for the specific barrier model considered in Ref. 5.

2. DERIVATION OF THE FUNDAMENTAL EQUATIONS

We assume for definiteness that local fluctuations in the impurity concentration $N(\mathbf{r})$ are responsible for the formation of the perforations. The specific transparency of the specimen is

$$\sigma_F = \frac{S_0}{S} \sum_i \Delta n_i \exp\{-v_i(F)\}, \quad (1)$$

where Δn_i is the number of perforations of the i th kind over the entire specimen [they are characterized by their concentration distribution $N_i(\mathbf{r})$, which is assumed known]; $\exp\{-v_i(F)\}$ is the transparency of perforations i for a specified external agent F ; S is the specimen area, and $S_0^{1/2}$ is the characteristic dimension of the perforations (S is given in units of S_0 in what follows). It is important to note that the perforations contributing the most to σ_F are separated by distances much greater than $S_0^{1/2}$, i.e., they are formed by different impurities. The probability of finding Δn_i perforations of type i in a specimen is therefore given by the Poisson distribution

$$p(\Delta n_i) = \frac{\exp(-\overline{\Delta n_i})}{(\Delta n_i)!} (\overline{\Delta n_i})^{\Delta n_i}, \quad (2)$$

where $\overline{\Delta n_i}$ is the mean number of perforations of type i present on a surface of area S . We use the formula

$$\sigma_F = e^{-Q} \quad (3)$$

for the specific transparency σ_F and define the DF for Q for a population of specimens by the formula

$$f_F(Q) = \left\langle \delta\left(Q + \ln\left\{\frac{1}{S} \sum_i \Delta n_i \exp[-v_i(F)]\right\}\right) \right\rangle, \quad (4)$$

where $\langle \dots \rangle$ denotes an average over specimens performed using the DF (2). Rewriting $f_F(Q)$ as

$$f_F(Q) = e^{-Q} \sum_{\Delta n_i=0}^{\infty} \delta\left(e^{-Q} - \frac{1}{S} \sum_i \Delta n_i \exp[-v_i(F)]\right) \times \prod_i p(\Delta n_i) \quad (5)$$

inserting (2), and replacing the δ -function by its Fourier expansion, we obtain

$$f_F(Q) = \frac{e^{-Q}}{2\pi} \int_{-\infty}^{\infty} dt \exp(it e^{-Q}) \sum_{\Delta n_i=0}^{\infty} \prod_i \exp(-\overline{\Delta n_i}) \times \frac{(\overline{\Delta n_i} \exp\{-(it/S) \exp[-v_i(F)]\})^{\Delta n_i}}{(\Delta n_i)!}. \quad (6)$$

The sums over Δn_i are easily calculated for each i .

$$f_F(Q) = \frac{e^{-Q}}{2\pi} \int_{-\infty}^{\infty} dt \exp(it e^{-Q}) \times \prod_i \exp\left[\overline{\Delta n_i} \left(\exp\left\{-\frac{it}{S} \exp[-v_i(F)]\right\} - 1\right)\right]. \quad (7)$$

The final expression for the DF is obtained by replacing the product in (7) by an integral over the argument of the exponential. The integration is over all impurity concentration fluctuations. The results can be expressed conveniently in terms of

$$\rho_F(u) = \int \delta(u - v\{N(\mathbf{r}), F\}) \exp(-\Omega\{N(\mathbf{r})\}) DN(\mathbf{r}), \quad (8)$$

the average concentration of perforations with a specified transparency logarithm u . Here $\exp\{-\Omega\{N(\mathbf{r})\}\}$ is the probability density for the formation of a fluctuation $N(\mathbf{r})$, and $\exp\{-v\{N(\mathbf{r}), F\}\}$ is the barrier transparency near the fluctuation. Expression (7) then becomes

$$f_F(Q) = \frac{e^{-Q}}{2\pi} \int_{-\infty}^{\infty} dt \exp\left\{ite^{-Q} + S \int_0^{\infty} du \rho_F(u) \times \left[\exp\left(-\frac{it}{S} e^{-u}\right) - 1\right]\right\}. \quad (9)$$

We will also be interested in the pair distribution function

$$\varphi_{F_1, F_2}(Q_1, Q_2) = \left\langle \delta\left(Q_1 + \ln\left\{\frac{1}{S} \sum_i \Delta n_i \exp[-v_i(F_1)]\right\}\right) \times \delta\left(Q_2 + \ln\left\{\frac{1}{S} \sum_j \Delta n_j \exp[-v_j(F_2)]\right\}\right) \right\rangle. \quad (10)$$

It describes how the transparency logarithms for a given specimen are correlated when F changes. An expression for $\varphi_{F_1, F_2}(Q_1, Q_2)$ can be derived from Eq. (10) by the same method used to obtain Eq. (9) for $f_F(Q)$ from (4):

$$\varphi_{F_1, F_2}(Q_1, Q_2) = \frac{\exp[-(Q_1 + Q_2)]}{(2\pi)^2} \int_{-\infty}^{\infty} dt_1 \int_{-\infty}^{\infty} dt_2 \times \exp(it_1 e^{-Q_1} + it_2 e^{-Q_2}) \chi_{F_1, F_2}(it_1, it_2), \quad (11)$$

where

$$\chi_{F_1, F_2}(x, y) = \exp\left\{S \int_0^{\infty} du_1 \int_0^{\infty} du_2 \rho_{F_1, F_2}(u_1, u_2) \times \left\{\exp\left[-\left(\frac{x}{S} e^{-u_1} + \frac{y}{S} e^{-u_2}\right)\right] - 1\right\}\right\}, \quad (12)$$

$$\rho_{F_1, F_2}(u_1, u_2) = \int \delta(u_1 - v\{N(\mathbf{r}), F_1\}) \delta(u_2 - v\{N(\mathbf{r}), F_2\}) \times \exp(-\Omega\{N(\mathbf{r})\}) DN(\mathbf{r}). \quad (13)$$

The correlation function for the transparency logarithm is

$$K(F_1, F_2) = \langle (\ln \sigma_{F_1} - \langle \ln \sigma_{F_1} \rangle) (\ln \sigma_{F_2} - \langle \ln \sigma_{F_2} \rangle) \rangle, \quad (14)$$

which can be expressed in terms of the function (12) as follows (see Appendix 1):

$$K(F_1, F_2) = \int_0^{\infty} \int_0^{\infty} \frac{dx dy}{xy} (\chi_{F_1, F_2}(x, y) - \chi_{F_1, F_2}(x, 0) \chi_{F_1, F_2}(0, y)). \quad (15)$$

Calculations based on Eqs. (9), (11) and (15) require that a specific barrier model be chosen. In this paper we consider a barrier in a p - n semiconductor junction, although we will see that the choice of model does not affect the qualitative results.

3. DESCRIPTION OF THE MODEL

Figure 1 shows the band diagram for a p - n junction. Interband tunneling of electrons is responsible for the current that flows when a large potential difference is applied

between the n - and p -type regions. Since there are no free electrons in the region $0 < x < x_c$, the distribution of charged impurities determines the shape of the barrier beneath which the electrons tunnel. The barrier height is fixed and equal to the gapwidth ε_g , however, its thickness may vary with fluctuations in the charged impurity concentration. These fluctuations are particularly important when the mean donor and acceptor concentrations \bar{N}_D and \bar{N}_A are nearly equal, i.e., the condition $\bar{N}_D - \bar{N}_A$ are nearly equal, i.e., the condition $\bar{N}_D - \bar{N}_A \ll \bar{N}_D + \bar{N}_A$ for strong compensation is satisfied; this is because the average barrier thickness depends on the difference $\bar{N}_D - \bar{N}_A$, while the thickness fluctuations depend on the sum $\bar{N}_D + \bar{N}_A$. Regions of high donor or low acceptor concentration where the barrier is much thinner than normal, can also act as perforations in this model. The electric field applied to the p - n junction serves as the external agent. It was shown in Ref. 5 that most of the contribution to the transparency comes from perforations that form due to gaussian fluctuations in the impurity concentration, i.e., fluctuations for which $N(\mathbf{r}) \ll \bar{N}_D, \bar{N}_A$, where $N(\mathbf{r}) = N_D(\mathbf{r}) - N_A(\mathbf{r}) - \bar{N}_D + \bar{N}_A$. In this case we have

$$\Omega\{N(\mathbf{r})\} = \frac{1}{2(\bar{N}_D + \bar{N}_A)} \int d^3r N^2(\mathbf{r}) \quad (16)$$

for the formation probability of a fluctuation $\exp(-\Omega)$. Let $V(\mathbf{r})$ be the component of the potential produced by the fluctuation $N(\mathbf{r})$; $V(\mathbf{r})$ and $N(\mathbf{r})$ are related by the Poisson equation. The logarithm of the electron tunneling probability is given by⁵

$$v\{N(\mathbf{r}), F\} = \left(\frac{8m}{\hbar^2 \varepsilon_g}\right)^{1/2} \int_0^{x_t} dx [(Fx - V(x))(V(x) - Fx + \varepsilon_g)]^{1/2}, \quad (17)$$

$$V(0) = 0, \quad V(x_t) = -\varepsilon_g + Fx_t,$$

where the integral is along the axis of the perforation and m is the effective electron mass. The quantity $\rho_F(u)$ can be found by substituting Eqs. (16), (17) into (8) and calculating the functional integral by the method of steepest descent. To find the result to exponential accuracy, one must find a distribution $\tilde{N}(\mathbf{r})$ minimizing Ω subject to the constraint $v\{N(\mathbf{r}), F\} = u$. A calculation similar to the one in Ref. 5 yields the result

$$\rho_F(u) = \exp\left(-\frac{Q_0^2}{4u} + \frac{Q_0 F}{F_0}\right), \quad (18)$$

where $Q_0 \ll 1$ is given by

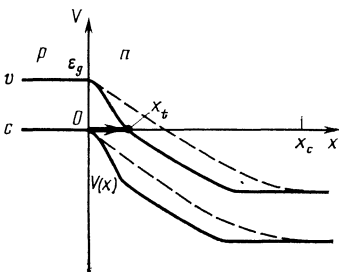


FIG. 1. Band diagram for a p - n junction. The positions of the top of the valence band (v) and the bottom of the conduction band (c) are shown near a puncture (solid line) and in the absence of fluctuations (dashed line). The arrow shows the tunneling path of the electron; x_t is the turning point.

$$Q_0 = \frac{\Gamma^2(1/4)}{24\pi} \left(\frac{\varepsilon_g}{E_B}\right)^{3/4} (\bar{N}_D + \bar{N}_A)^{-1/2} a_B^{-3/4}, \quad (19)$$

Here $a_B = \hbar^2 \kappa / m e^2$ and $E_B = m e^4 / 2 \hbar^2 \kappa^2$ are the Bohr radius and electron energy, κ is the dielectric constant, and the characteristic electric field is

$$F_0 = \frac{2\Gamma^2(1/4)}{3} \varepsilon_g^{1/4} E_B^{3/4} (\bar{N}_D + \bar{N}_A)^{1/2} a_B^{1/2}. \quad (20)$$

Formula (18) is valid when $F \ll F_0$; a qualitative derivation of (18) for $F = 0$ is given in Appendix 2.

In our model the function (13), which will be used to calculate the transparency logarithm correlation function (15), is equal to

$$\rho_{F_1, F_2}(u_1, u_2) = \rho_{\bar{F}}(\bar{u}) \left(\frac{Q_0 H}{\pi}\right)^{1/2} \frac{F_0}{\delta F \bar{u}} \times \exp\left[-\frac{Q_0 H}{\bar{u}^2} \left(\frac{F_0}{\delta F}\right)^2 \left(\delta u + 4\frac{\bar{u}^2 \delta F}{Q_0 F_0}\right)^2\right], \quad (21)$$

where $\bar{F} = (F_1 + F_2)/2$, $\bar{u} = (u_1 + u_2)/2$, $\delta F = F_1 - F_2$, $\delta u = u_1 - u_2$, and H is the dimensionless ratio \bar{F}/F_0 . Expression (21) is valid when $\delta u \ll \bar{u}$, $\delta F \ll \bar{F}$, in which case the concentration fluctuations $N(\mathbf{r})$ contributing most to the functional integral (13) differ only slightly from the optimum fluctuation determining the function $\rho_F(u)$ in (8). We have used this fact in deriving Eq. (21), which shows that for perforations with transparency $\exp(-\bar{u})$ in a field \bar{F} , the change δF in the field is described by a gaussian distribution peaking at δu , where δu is equal to the change in the transparency logarithm for a perforation which is optimal at $F = \bar{F}$ and $u = \bar{u}$.

The width of this distribution is of the order of $\bar{u} \delta F / F_0 (Q_0 H)^{1/2}$ and depends on H . We have $H \sim 1$ when $F \sim F_0$; however, when calculating H for $F \ll F_0$ it is important to note that the potential distribution $V(x)$ on the axis of an optimum perforation (Fig. 1) is of the form $V(x) + \varepsilon_g \sim (x_t - x)^{4/3}$ for $F \rightarrow 0$ and $x_t - x \ll x_t$ (Ref. 5); the electric field therefore vanishes as $(x_t - x)^{1/3}$ when $x \rightarrow x_t$. A small region $x_t - x \ll x_t$ of the perforation is thus most sensitive to changes in the external field, and fluctuations of the charged impurity concentration in this region therefore give the dominant contribution to the characteristic spread in δu and hence to H . This contribution increases as $x_t - x$ decreases and depends on the minimum value $x_t - x = \tilde{x}_t$ determined by the requirement that the fluctuation charge in a region of volume \tilde{x}^3 near $x = x_t$ cannot be less than the charge of one electron. In this case one finds that H is much less than unity and is equal in order of magnitude to $(F/F_0)^3$ for $F \gg \bar{F}$ and to $(\bar{F}/F_0)^3$ for $F \ll \bar{F}$, where

$$\bar{F} = F_0 Q_0^{-1/3} (Q_0/\bar{u})^{2/21} (\bar{N}_D a_B^3)^{-1/21} \ll F_0.$$

4. QUALITATIVE ANALYSIS

We first consider the case of zero applied field $F = 0$. The specific transparency averaged over a population of specimens is given by the contribution from all the perforations,

$$\sigma = \int_0^\infty du g(u), \quad (22)$$

where

$$g(u) = e^{-u} \rho_0(u) = \exp(-u - Q_0^2/4u), \quad (23)$$

and is equal to the perforation transparency u times the concentration of perforations with transparency u [Eq. (18)]. Since the integrand $g(u)$ is sharply peaked at $u = u_{opt} = Q_0/2 \gg 1$ with width $|u - Q_0/2| \sim Q_0^{1/2}$, the average transparency is determined primarily by the optimum perforations with transparency $\exp(-Q_0/2)$ and is equal to

$$\sigma = Q_0^{1/2} e^{-Q_0/2} \quad (24)$$

(numerical factors multiplying the exponentials will be neglected in this section). The derivation of (24) assumes that the specimen area S is exponentially large, so that the number of optimum perforations in the specimens is also large. This condition can be expressed as

$$S \rho_0(u_{opt}) \gg 1. \quad (25)$$

Introducing the parameter

$$\nu = \frac{\ln S}{|\ln \rho_0(u_{opt})|} = \frac{2}{Q_0} \ln S \quad (26)$$

we can rewrite (25) as $\exp[Q_0(\nu - 1)/2] \gg 1$, which for $Q_0 \gg 1$ reduces to the condition $\nu > 1$. If (25) fails ($\nu < 1$) then most specimens will not contain even a single optimum perforation, and in this case the few perforations with the largest transparency will give the dominant contribution to the specific transparency. This means that when calculating the specific transparency for a typical specimen, we must take the lower limit of the integral in (22) to be $u = u_f$, where u_f is given by the conditions $S \rho_0(u_f) \sim 1$, so that $\exp(-u_f)$ is the maximum transparency of the perforations in a typical specimen. Recalling the definition (26), we obtain

$$u_f = Q_0/2\nu. \quad (27)$$

Since the integral (22) in this case is determined by the value of the integrand at $u = u_f$, we have

$$\sigma = \frac{1}{1-\nu^2} \exp\left\{-\frac{Q_0}{2}\left(\nu + \frac{1}{\nu}\right)\right\} \quad (28)$$

for the specific transparency of a typical specimen. This expression agrees with (24) when $\nu = 1$ (more precisely, when $1 - \nu \sim Q_0^{-1/2}$).

Expressions (28) and (24) give the specific transparency for typical specimens of small and large area. Actually, however, as has already been stated in the Introduction, the transparency fluctuates from one specimen to another. An exact expression for the DF of the logarithm of the specific transparency was given above in Eq. (9), Sec. 2. Expressions (24) and (28) specify the position of the maximum of the DF. In this section we analyze qualitatively how the width of the distribution function depends on the parameter ν . The large-area case $\nu > 1$ will be considered first. The specific transparency of a given specimen is a random variable described by Eq. (1). Since the perforations are distributed randomly and independently, the variance of the transparency can be calculated without difficulty:

$$\langle (\delta\sigma)^2 \rangle = \frac{1}{S^2} \sum_i \langle (\delta(\Delta n_i))^2 \rangle \exp(-2u_i), \quad (29)$$

where $\delta(\Delta n_i)$ is the fluctuation in the number of perforations of type i . Since the distribution of Δn_i over the specimens is given by the Poisson formula (2), we have

$$\langle (\delta(\Delta n_i))^2 \rangle = \overline{\Delta n_i} = S \rho_0(u_i). \quad (30)$$

Inserting (30) into (29) and replacing the sum by an integration, we get

$$\langle (\delta\sigma)^2 \rangle = \int_0^\infty du h(u), \quad (31)$$

where the function

$$h(u) = \exp\left(-\frac{\nu Q_0}{2} - \frac{Q_0^2}{4u} - 2u\right) \quad (32)$$

gives the contribution to $\langle (\delta\sigma)^2 \rangle$ from perforations with transparency e^{-u} . Since $h(u)$ peaks sharply at $u = Q_0/2^{3/2}$, with width $\sim Q_0^{1/2}$, most of the contribution to $\langle (\delta\sigma)^2 \rangle$ comes from perforations whose transparency is much greater than for the perforations determining the average transparency, for which $u = Q_0/2$. Evaluating the integral in (31), we obtain

$$\langle (\delta\sigma)^2 \rangle = Q_0^{1/2} \exp[-Q_0(\nu/2 + 2^{1/2})]. \quad (33)$$

The width ΔQ of the DF for the logarithm of the specific transparency is equal to the ratio $[\langle (\delta\sigma)^2 \rangle]^{1/2}/\sigma$, apart from a numerical factor; using Eqs. (24) and (33) we thus get

$$\Delta Q = Q_0^{-1/4} \exp[-1/4 Q_0(\nu - 4 + 2^{1/2})]. \quad (34)$$

The width of the distribution function is seen to be inversely proportional to $S^{1/2}$. The above analysis is valid only when the number of perforations contributing to the variance is large. Since this number is

$$S \rho_0\left(\frac{Q_0}{2^{1/2}}\right) = \exp\left[\frac{Q_0}{2}(\nu - 2^{1/2})\right], \quad (35)$$

Eq. (34) can be used when $\nu > 2^{1/2}$. Although Eq. (31) for the variance remains correct for $1 < \nu < 2^{1/2}$, the principal contribution in this case comes from exceptional specimens that contain perforations with $u = Q_0/2^{3/2}$ (the number of such specimens is exponentially small). However, since the width of the distribution function is determined by the typical specimens, it can be calculated by considering only the perforations present in such specimens. This is equivalent to replacing the lower limit of the integral in (31) by u_f given by Eq. (27). The width of the DF for the logarithm of the specific transparency is found to be

$$\begin{aligned} \Delta Q &= \frac{1}{\sigma} \left(\int_{u_f}^\infty du h(u) \right)^{1/2} \\ &= [\sigma(2-\nu^2)^{-1/2}]^{-1} \exp\left[-\frac{Q_0}{2}\left(\nu + \frac{1}{\nu}\right)\right], \end{aligned} \quad (36)$$

which upon substitution of (24) becomes

$$\Delta Q = [Q_0(2-\nu^2)]^{-1/2} \exp\left[-\frac{Q_0}{2}\left(\nu + \frac{1}{\nu} - 2\right)\right]. \quad (37)$$

We see that as the area increases, the narrowing of the DF is much slower than predicted by Eq. (34). Equation (36) remains valid for $\nu < 1$, provided Eq. (28) is used for the specific transparency σ . The result is

$$\Delta Q = 1 - \nu^2. \quad (38)$$

The above analysis breaks down for $\nu \ll 1$, for which the fluctuations in u_f from specimen to specimen become important near the value $Q_0/2\nu$. It is clear from the definition of u_f that these fluctuations have the characteristic scale

$$\left(S \frac{d\rho_0}{du}(u_i) \right)^{-1} \sim \frac{1}{\nu^2}.$$

Since $|\ln\sigma|$ for $\nu \ll 1$ is nearly equal to u_f [Eq. (27)], the fluctuations in $|\ln\sigma|$, and hence also the width of the DF, are of order $1/\nu^2$ for $\nu \ll 1$.

We have thus far considered the case of zero applied field. According to Eq. (18), the concentration of perforations with a specified transparency e^{-u} increases with the applied field. This is because the field enhances the transparency of all of the perforations. Indeed, perforations with transparency e^{-u} at a given field F would be less transparent at $F = 0$, and hence more numerous, than perforations with transparency e^{-u} in zero field. To calculate the average specific transparency for $F \neq 0$ in the large-area case ($\nu > 1$), one must replace $\rho_0(u)$ by $\rho_F(u)$ in (23). One finds that the optimum perforations again correspond to $u = Q_0/2$, and hence the average specific transparency is

$$\sigma_F = Q_0^{1/2} \exp(-Q_0 + Q_0 F/F_0). \quad (39)$$

For small areas ($\nu < 1$) the transparency for $F \neq 0$ is determined by the perforations for which $S\rho_F(u) \sim 1$, whence we find from Eqs. (18) and (26) that

$$u_i(F) = Q_0 [2(\nu + 2F/F_0)]^{-1}. \quad (40)$$

The specific transparency for a typical specimen is then

$$\sigma_F = \frac{1}{S} \exp[-u_i(F)] = \exp\left[-\frac{Q_0}{2}\left(\nu + \frac{1}{\nu}\right) + \frac{Q_0 F}{\nu^2 F_0}\right]. \quad (41)$$

In addition to increasing the transparency, the applied field also narrows the distribution function. Here the range of areas $|\nu - 1| \ll 1$ is of greatest interest, since a small change in the field suffices to replace large fluctuations ($\nu < 1$) by small ones ($\nu > 1$) in a given population of specimens. Indeed, $S\rho_F(u_{\text{opt}}) \gg 1$ is the condition for the fluctuations to be small; using Eqs. (18) and (26), we can rewrite it in the form $\nu > 1 - 2F/F_0$. For $F \neq 0$ this inequality can clearly be satisfied even when $\nu < 1$, i.e., when large-fluctuation behavior occurs at zero field. As was pointed out above, Eqs. (24) and (28) imply that the interval of ν values over which the transition from large to small fluctuations occurs is of length $\sim Q_0^{-1/2}$, which corresponds to

$$|F - (1 - \nu)F_0/2| \sim F_0/Q_0^{1/2}$$

in terms of the external field. In terms of its effect on the transparency, the applied field is thus equivalent to an exponentially large increase in the effective area of the specimens.

We will now consider another consequence of the influence of the external field on the transparency of the perforations: The logarithm of the transparency of the specimen oscillates as a function of F about the mean value given by (41). We will show this for the small-area case ($\nu < 1$), which is of greatest interest. We assume for simplicity that for some initial external field $F = F^*$, the main contribution to the transparency of the specimen comes from only two

perforations A and B of maximum transparency. The difference between the transparency logarithm for these perforations in a typical specimen is of order $1/\nu^2$, which for $\nu \lesssim 1$ is comparable to the width of the DF for the transparency logarithm. The perforations A and B both become more transparent when the external field is increased by δF . According to Eq. (21), the change in the transparency logarithm for each perforation is expressible as the sum of a regular component $\delta u = -4u_i^2 \delta F/F_0 Q_0$, which is the same for both perforations, plus a random component described by a gaussian distribution of characteristic width

$$\delta u' \sim u_i \delta F/F_0 (Q_0 H)^{1/2}.$$

If δF is sufficiently small, the random component in the transparency logarithm has little effect on the ratio of the transparencies for perforations A and B . However, for

$$\delta F \sim F_0 (Q_0 H)^{1/2} / u_i \nu^2 = \delta F_c,$$

we have $\delta u' \sim 1/\nu^2$ so that, roughly speaking, half of the time perforation B "overtakes" A when F increases by δF_c , i.e., it becomes more transparent than A even though it was less transparent initially. As F increases further, a new perforation C overtakes perforation A , the transparency of the specimen is determined by the sum of the transparencies of perforations B and C , and the entire process is repeated. The transparency logarithm thus oscillates with characteristic period δF_c and amplitude comparable to the width of the distribution function. These oscillations are shown schematically in Fig. 2.

One can show that for specimens of large area ($\nu > 1$), the logarithm of the transparency should also oscillate with the same period δF_c over the width of the distribution function. The oscillations in this case are due not to competition among the perforations determining the transparency logarithm but rather to competitions among the much more transparent perforations that determine the width of the distribution function.

The above explanation might appear to be inconsistent. Indeed, the successive overtakings should cause the transparency logarithm to grow at an ever-increasing rate, whereas Eq. (41) predicts that the mean value about which the oscillations occur should depend linearly on the external field. In fact, however, the slopes $\partial |\ln\sigma|/\partial F$ of the transparency logarithms decrease with F for all of the perforations considered above, and one can show that on the average this completely cancels the faster-than-linear increase due to the overtakings.

We have seen that the transparency is determined by perforations which are newly formed when the external field

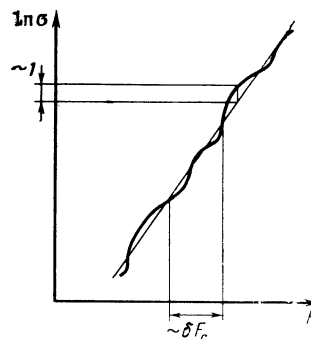


FIG. 2.

changes; since different perforations form in regions of high impurity concentration which are remote from one another, this can be regarded equivalently as a reconfiguration of the impurities in the specimen, i.e., as a replacement of an old specimen by a new one. In this sense the oscillations are analogous to the mesoscopic oscillations in the hopping and metallic conductivities of a small-area specimen when the magnetic field changes; these oscillations are caused by interference effects associated with multiple electron scattering.⁷⁻⁹ We note that in our case, the typical sample dimensions for which the oscillations can be observed are exponentially large.

5. DERIVATION OF EXPRESSIONS FOR THE DISTRIBUTION FUNCTION

We will carry out the calculations for the zero-field case, $F = 0$. Substituting expression (18) for $\rho_0(u)$ into (9), we can rewrite the distribution function as

$$f(Q) = \frac{e^{-Q}}{2\pi} \int_{-\infty}^{\infty} dt \exp[ite^{-Q} + I_\nu(t)], \quad (42)$$

$$I_\nu(t) = \int_0^{\infty} du \exp \left[\frac{Q_0}{2} \left(\nu - \frac{Q_0}{2u} \right) \right] \times \left\{ \exp \left\{ -it \exp \left[- \left(u + \frac{\nu Q_0}{2} \right) \right] \right\} - 1 \right\}. \quad (43)$$

We first assume that $\nu < 1$. According to Eqs. (27), (28) in Sec. 4, Q and u in this case are nearly equal to $Q_0(\nu + 1)/\nu/2$ and $Q_0/2\nu$, respectively. It is therefore convenient to make the following change of variables in the integrals in (42) and (43):

$$t = \nu \exp \left[\frac{Q_0}{2} \left(\nu + \frac{1}{\nu} \right) \right], \quad (44)$$

$$u = Q_0/2\nu + u'. \quad (45)$$

Since u' is typically much less than Q_0 , the exponential in the first factor in (43) can be expanded to second order in the small parameter u'/Q_0 , and the integral (43) becomes

$$I_\nu = \int_{-\infty}^{\infty} du' \exp \left(\nu^2 u' - \frac{2\nu^3}{Q_0} u'^2 \right) [\exp(-ive^{-u'}) - 1]. \quad (46)$$

The evaluation of (46) depends on the range over which ν varies:

$$I_\nu = - \frac{\Gamma(1-\nu^2)}{\nu^2} \exp \left(\frac{i\pi\nu^2}{2} \right) \nu^{\nu^2}, \quad |1-\nu| \gg Q_0^{-1/2}, \quad (47a)$$

$$I_\nu = - \frac{\pi\nu}{2} + i\nu \left[\ln \nu - \left(\frac{\pi Q_0}{2} \right)^{1/2} \exp \left[\frac{Q_0}{2} (\nu-1)^2 \right] \times \Phi \left(\frac{Q_0^{1/2}}{2^{1/2}} (1-\nu) \right) \right], \quad |1-\nu| \ll Q_0^{-1/2}, \quad (47b)$$

where

$$\Phi(x) = \pi^{-1/2} \int_x^{\infty} dw \exp(-w^2) \quad (48)$$

is the error integral. Formula (47a) follows by neglecting the second term in the argument of the exponential in (46), so that the integral reduces to the Γ -function. The real part

of (47b) follows in precisely the same way. The imaginary part of (47b) can be found by expanding the exponential in the second factor in (46) and replacing the lower limit of integration by $u = \ln \nu$. Formulas (47a) and (47b) assume that $\nu > 0$, which is no restriction since it is clear from (46) that $I_\nu(-\nu) = I_\nu^*(\nu)$. The final expression for the distribution function follows upon inserting (47a) and (47b) into (42). For the case $1 - \nu \gg Q_0^{-1/2}$ it is convenient to center the distribution function near $Q = Q_0(\nu + 1/\nu)/2$ by introducing the quantity

$$\Delta = Q - \frac{Q_0}{2} \left(\nu + \frac{1}{\nu} \right) + \frac{1}{\nu^2} \ln \frac{\Gamma(1-\nu^2)}{\nu^2}. \quad (49)$$

Making the change of variable $x = \nu [\Gamma(1-\nu^2) \nu^2]^{1/\nu^2}$, we obtain

$$f(Q) = \frac{e^{-\Delta}}{\pi} \int_0^{\infty} dx \exp \left(-x^{\nu^2} \cos \frac{\pi\nu^2}{2} \right) \cos \left(x e^{-\Delta} - x^{\nu^2} \sin \frac{\pi\nu^2}{2} \right). \quad (50)$$

Figure 3a shows the function f calculated numerically for several values of ν . For large positive and negative Δ we have the asymptotic formulas

$$f(Q) = \left[\frac{\gamma\beta(\beta+1)}{2\pi} \right]^{1/2} \exp \left(\frac{\beta\Delta}{2} - \gamma e^{\beta\Delta} \right), \quad \Delta \gg 1, \quad (51a)$$

$$f(Q) = \frac{\sin \pi\nu^2}{\pi} \Gamma(\nu^2+1) e^{\Delta\nu^2}, \quad \Delta < 0, \quad |\Delta| \gg 1, \quad (51b)$$

where

$$\beta = \nu^2 / (1-\nu^2), \quad \gamma = (1-\nu^2) (\nu^2)^{\nu^2/(1-\nu^2)}. \quad (52)$$

The derivation of Eqs. (51) is given in Appendix 3.

As shown in Appendix 3, for $\nu \ll 1$ the expression for the distribution function simplifies to

$$f(Q) = \nu^2 \exp(\Delta\nu^2 - e^{\Delta\nu^2}). \quad (53)$$

We see that the width of the DF increases as $1/\nu^2$ as ν de-

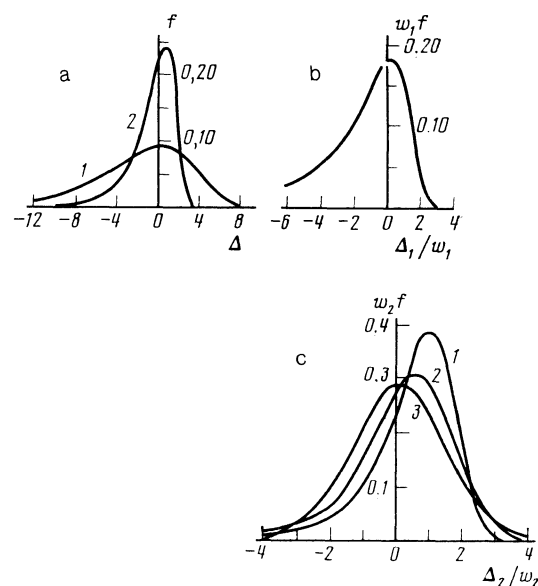


FIG. 3. Distribution function for the logarithm of the specific transparency for several values of the parameter ν : a: 1) 0.5; 2) 0.707; b: 1) 1.0; 2) 1.3; 3) 1.4. The distributions were calculated by Eqs. (50), (56), and (62), respectively.

creases, in agreement with the results of our qualitative analysis. For the case $|1 - \nu| \ll Q_0^{-1/2}$ we find upon inserting (47b) in (42) and writing

$$\Delta_1 = Q - Q_0 + \ln \left[\left(\frac{\pi Q_0}{2} \right)^{1/2} \Phi \left(\frac{Q_0^{1/2}}{2^{1/2}} (1 - \nu) \right) \right], \quad (54)$$

$$w_1 = \left[\left(\frac{\pi Q_0}{2} \right)^{1/2} \exp \left[\frac{Q_0}{2} (1 - \nu)^2 \right] \Phi \left(\frac{Q_0^{1/2}}{2^{1/2}} (1 - \nu) \right) \right]^{-1}, \quad (55)$$

that the distribution function is

$$f(Q) = \frac{1}{\pi w_1} \int_0^\infty dv e^{-\pi v^2/2} \cos \left(v \frac{\Delta_1}{w_1} - v \ln v \right), \quad |1 - \nu| \ll Q_0^{-1/2}, \quad (56)$$

which is plotted in Fig. 3b. For large negative mismatches $\Delta_1 < 0$, $|\Delta_1| \gg w_1$, $f(Q)$ decays as w_1/Δ_1^2 , while for $\Delta_1 \gg w_1$ it falls off as $\exp[-\exp(\Delta_1/w_1)]$. The distribution function (56) has width $\sim w_1$, for which we have the asymptotic formulas

$$w_1 = 2(1 - \nu), \quad 1 - \nu \gg Q_0^{-1/2}, \\ w_1 = \left(\frac{2}{\pi Q_0} \right)^{1/2} \exp \left[-\frac{Q_0}{2} (1 - \nu)^2 \right], \quad \nu - 1 \gg Q_0^{-1/2} \quad (57)$$

in the two limiting cases, in agreement with the results (37), (38) of the qualitative analysis. Expression (55) for w_1 can be used to analyze how the distribution function becomes narrower as one goes from large ($\nu < 1$) to small ($\nu > 1$) fluctuations.

An expression for the width of the DF for $|\nu - 1| \ll 1$ in a finite field F can be obtained by replacing ν in Eq. (55) by $\nu + 2F/F_0$. This can be seen formally by replacing $\rho_0(u)$ in (43) by $\rho_F(u)$ and carrying out calculations similar to the ones above. Thus, as was already noted in Sec. 4, the transition from large to small fluctuations can be accomplished by changing the external field.

We next examine the case $\nu > 1$, for which the width of the distribution is determined by the values $u \approx Q_0/2\nu$ and the position of the maximum by the values $u \approx Q_0/2$. Expression (46) for I_ν was derived under the assumption that $|u - Q_0/2\nu| \ll Q_0$. Since this does not hold in the present case, we must first separate out the contribution from $u \approx Q_0/2$ in the integral (43); this contribution is a sum of two terms:

$$I_\nu = I_\nu^{(1)} + I_\nu^{(2)}, \\ I_\nu^{(1)} = -iv \exp \left[\frac{Q_0}{2} \left(\nu + \frac{1}{\nu} \right) \right] \int_0^\infty du \exp \left(-u - \frac{Q_0^2}{4u} \right), \quad (58)$$

$$I_\nu^{(2)} = \int_{-\infty}^\infty du' \exp \left(\nu^2 u' - \frac{2\nu^3 u'^2}{Q_0} \right) [\exp(-ive^{-u'}) + ive^{-u'} - 1], \quad (59)$$

where u' and v are related to u and t by Eqs. (44) and (45). Since the integrand in (58) is sharply peaked at $u = Q_0/2$, the integral is readily evaluated by the method of steepest descent:

$$I_\nu^{(1)} = -iv \left(\frac{\pi Q_0}{2} \right)^{1/2} \exp \left[\frac{Q_0}{2} \left(\nu + \frac{1}{\nu} - 2 \right) \right]. \quad (60)$$

Since the integral for $I_\nu^{(2)}$ converges for $|u'| \ll Q_0$, in deriving

(59) we have expanded the exponential in the first factor in (43) in powers of the parameter u'/Q_0 . As in the case of (46), the evaluation of the integral (59) depends on ν :

$$I_\nu^{(2)} = \exp \left(\frac{i\pi\nu^2}{2} \right) \frac{\Gamma(2 - \nu^2)}{\nu^2(\nu^2 - 1)} \nu^{\nu^2}, \quad 2^{1/2} - \nu \gg Q_0^{-1/2}, \quad (61a)$$

$$I_\nu^{(2)} = -\nu^2 \frac{(\pi Q_0)^{1/2}}{2^{3/4}} \exp \left[\frac{Q_0(2^{1/2} - \nu)^2}{2^{1/2}} \right] \\ \times \Phi \left(\frac{Q_0^{1/2}}{2^{3/4}} (2^{1/2} - \nu) \right), \quad |2^{1/2} - \nu| \ll Q_0^{-1/2}. \quad (61b)$$

Expression (61a) and (61b) follow from (59) in exactly the same way as (47a) and (47b) follow from (46). Substituting the sum of (60) and (61a) into (42) and making the change of variable

$$x = \nu [\Gamma(2 - \nu^2)/\nu^2(\nu^2 - 1)]^{1/\nu^2}$$

we obtain

$$f(Q) = \frac{1}{\pi w_2} \int_0^\infty dx \exp \left(x^{\nu^2} \cos \frac{\pi\nu^2}{2} \right) \cos \left(x \frac{\Delta_2}{w_2} - x^{\nu^2} \sin \frac{\pi\nu^2}{2} \right), \\ 2^{1/2} - \nu \gg Q_0^{-1/2}, \quad (62)$$

for the distribution function $f(Q)$, where

$$\Delta_2 = Q - Q_0 + \ln(\pi Q_0/2)^{1/2}, \quad (63)$$

$$w_2 = \left(\frac{2}{\pi Q_0} \right)^{1/2} \left(\frac{\Gamma(2 - \nu^2)}{\nu^2(\nu^2 - 1)} \right)^{1/\nu^2} \exp \left[-\frac{Q_0}{2} \left(\nu + \frac{1}{\nu} - 2 \right) \right]. \quad (64)$$

Equation (63) shows that the DF is centered at $Q \approx Q_0$ and has width $\sim w_2$, in agreement with Eqs. (24), (37) from the qualitative analysis. Figure 3c plots the distribution function for several values of ν .

For $|\nu - 2^{1/2}| \ll Q_0^{-1/3}$ the integral in (42) can easily be evaluated by substituting the sum of expressions (60) and (61b). The resulting distribution function is gaussian:

$$f(Q) = [(2\pi)^{1/2} w_3]^{-1} \exp(-\Delta_2^2/2w_3^2) \quad (65)$$

with width

$$w_3 = 2^{-1/\nu} (\pi Q_0)^{-1/\nu} \exp \left[-\frac{Q_0}{4} (\nu - 4 + 2^{3/2}) \right] \Phi^{1/2} \left[\frac{Q_0^{1/2}}{2^{3/4}} (2^{1/2} - \nu) \right]. \quad (66)$$

Expression (65) is in fact valid for all $\nu > 2^{1/2}$, as is readily seen by expanding the integrand in (43) through second order in t , after which the integrals in (43) and (42) are easily evaluated. Expression (66) for the width of the DF simplifies for $\nu - 2^{1/2} \gg Q_0^{-1/2}$:

$$w_3 = 2^{-1/\nu} (\pi Q_0)^{-1/\nu} \exp \left[-1/4 Q_0 (\nu - 4 + 2^{3/2}) \right] \quad (67)$$

which agrees with Eq. (34) in Sec. 4 up to a numerical coefficient.

6. CALCULATION OF THE CORRELATION FUNCTION FOR THE LOGARITHM OF THE TRANSPARENCY

As already stated in the Introduction, the amplitude and period of the transparency oscillations are characterized quantitatively by the correlation function for the transpar-

ency logarithm. To calculate the correlation function using Eq. (15), one must first derive an expression for the function $\chi_{F_1, F_2}(x, y)$ by substituting expression (21) for $\rho_{F_1, F_2}(u_1, u_2)$ into Eq. (12). Since the oscillations should be largest for small specimens ($\nu < 1$), we will do the calculations for this case. We showed in Sec. 4 that for $\nu < 1$ the transparency of a typical specimen is determined by perforations for which $u = Q_0/2(\nu + 2F/F_0)$. It is therefore helpful to replace \bar{u} in expression (21) for $\rho_{F_1, F_2}(u_1, u_2)$ by the variable $u' = \bar{u}Q_0/2(\nu + 2F/F_0)$ and expand in terms of the small parameter u'/Q_0 . This gives

$$\rho_{F_1, F_2} = \exp\left(-\frac{\nu Q_0}{2} + \nu^2 u'\right) \left\{ \left(\frac{4H}{\pi Q_0}\right)^{1/2} \frac{\nu F_0}{\delta F} \times \exp\left[-\frac{4\nu^2 H F_0^2}{Q_0 (\delta F)^2} \left(\delta u + \frac{Q_0 \delta F}{\nu^2 F_0}\right)^2\right] \right\}, \quad (68)$$

which upon substitution in (12) yields the following expression for χ :

$$\chi_{F_1, F_2}(x, y) = \exp\left\{ \left(\frac{4H}{\pi Q_0}\right)^{1/2} \frac{\nu F_0}{\delta F} \int_{-\infty}^{\infty} dv \exp\left[-\frac{4\nu^2 H F_0^2}{Q_0 (\delta F)^2} v^2\right] \times \int_{-\infty}^{\infty} du' e^{\nu^2 u'} \{ \exp[-e^{-u'}(x' e^{-\nu/2} + y' e^{\nu/2})] - 1 \} \right\}. \quad (69)$$

Here we have written

$$x' = x \exp\left[-\frac{Q_0}{2} \left(\nu + \frac{1}{\nu + 2F/F_0}\right) + \frac{Q_0 \delta F}{2\nu^2 F_0}\right], \quad (70)$$

$$y' = y \exp\left[-\frac{Q_0}{2} \left(\nu + \frac{1}{\nu + 2F/F_0}\right) - \frac{Q_0 \delta F}{2\nu^2 F_0}\right] \quad (71)$$

and replaced the variables of integration u_1, u_2 by u' and $v = \delta u + Q_0 \delta F / F_0 \nu^2$. The integral over du' was already evaluated in Sec. 5 in the derivation of Eq. (47a) from (46). Because of the integration, the function $\chi_{F_1, F_2}(x, y)$ becomes dependent on the arguments x', y' , as well as on the parameters ν and

$$\tau = \frac{\nu}{4} \left(\frac{Q_0}{H}\right)^{1/2} \frac{\delta F}{F_0} \quad (72)$$

and is given by the following expression:

$$\chi_\tau(x', y') = \exp\left\{ -\frac{\Gamma(1-\nu^2)}{\pi^{1/2} \nu^2} \int_{-\infty}^{\infty} dt e^{-t^2} (x' e^{-t/\nu^2} + y' e^{t/\nu^2})^2 \right\}. \quad (73)$$

Substituting (73) into (15) and integrating with respect to x', y' instead of x, y (this does not change the form of the correlation function), we obtain

$$K(\tau) = \int_0^\infty \int_0^\infty \frac{dx' dy'}{x' y'} [\chi_\tau(x', y') - \chi_\tau(x', 0) \chi_\tau(0, y')]. \quad (74)$$

It is clear from expressions (73) and (74) that the correlation function for the transparency logarithm is a function of the argument τ and decays with a single characteristic scale $\tau \sim 1$, which corresponds to a change $\delta F \sim F_0 (H / Q_0 \nu^2)^{1/2}$ in the external field. This result agrees with the characteristic period of the oscillations in the transparency logarithm found in the qualitative analysis.

One of the integrals in (74) (e.g., the one over x') can be evaluated explicitly by making the change of variable

$y' = x'v$. Since the integrals of the two terms taken separately diverge, it is convenient to first replace the product $x'y'$ in the denominator in (74) by $(x'y')^{1-\delta}$ and then let $\delta \rightarrow 0$ in the final result. We then obtain

$$K(\tau) = \frac{\pi^2}{6} \left(\frac{1}{\nu^4} - 1\right) - \frac{1}{\nu^2} \int_0^\infty \frac{dv}{v} \ln \left[\frac{J_\tau(v)}{(1+\nu)^{\nu^2}} \right], \quad (75)$$

$$J_\tau(v) = \frac{e^{-\tau^2/4}}{\pi^{1/2}} \int_{-\infty}^{\infty} dt e^{-t^2} (e^{-t/\nu^2} + \nu e^{t/\nu^2})^{\nu^2}. \quad (76)$$

The results from a numerical calculation of the correlation function $K(\tau)$ are shown in Fig. 4. We have the asymptotic formulas

$$K(\tau) = \frac{\pi^2}{6} \left(\frac{1}{\nu^4} - 1\right) - \frac{1-\nu^2}{\nu^4} \tau^2, \quad |\tau| \ll 1, \quad (77)$$

$$K(\tau) = \frac{2\pi^{1/2} \Gamma^2(1-\nu^2/2)}{\nu^4 \Gamma(1-\nu^2)} \frac{e^{-\tau^2/4}}{|\tau|}, \quad |\tau| \gg 1.$$

The first formula (for small τ) follows by expanding (76) to second order in τ ; the second follows by using the fact that for $|\tau| \gg 1$, the integrand in (76) has two well-separated maxima at $t = \pm \tau/2$.

7. CONCLUSIONS

All the results in this paper were derived for the specific barrier model considered in Ref. 5. A similar analysis can be given for the models in Refs. 1–4, 6, of which the ones in Refs. 1, 2 resemble the model considered here most closely. In both of those models, one studies the transmission of electrons across a dielectric film containing randomly distributed neutral impurities whose energies are nearly equal to the electron tunneling energy. The model in Ref. 1 assumes that the impurity levels have a nonzero energy spread, and that the electrons move by tunnel hopping from one impurity to the next. Isolated impurity chains that connect the opposite sides of the film, and in which the distance between the impurities is much less than the characteristic hopping length in the bulk material, serve as the perforations in this case. In the model in Ref. 2, all the impurity levels are assumed to lie at the same energy, while the energy of the oncoming electrons is uniformly distributed throughout some interval. In this case the electron transmission involves resonant tunnel-

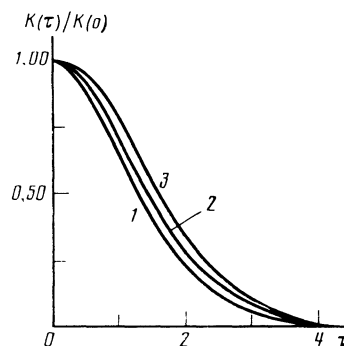


FIG. 4. Plot of the correlation function for the logarithm of the specific transparency [Eq. (75)] for three values of ν : 1) 0.0; 2) 0.75; 3) 1.0.

ing through the impurity levels, and the perforations consist of sparse chains of equidistant impurities which form an energy band whose transmission coefficient is close to unity. The optimum chains in Ref. 2 are the one for which the band width times the formation probability is a maximum. The results in the present paper concerning the distribution function for the transparency logarithm all carry over to these models without change, provided Q_0 is taken equal to the logarithm of the specific transparency in the large-area limit¹⁾ and Eq. (26) is used for ν .

Two other models were considered in Refs. 3 and 6. Electron tunneling through a film was considered in Ref. 3, the film acting as a barrier of constant height. Owing to the surface roughness of the film, the electron tunneling length, and hence the tunneling transparency, fluctuates along the plane of the barrier. The perforations consist of exponentially infrequent narrow regions, and a potential difference between the two sides of the film can serve as the external agent. A system of isolated filaments containing randomly distributed impurities acting as absorbing centers was considered in Ref. 6. Although the filament transparency increases exponentially as the number of impurities decreases, the number of perforations (filaments with only a few impurities) is exponentially small. The wave transmission coefficient through an individual impurity is the only parameter that can be manipulated externally. The models in Refs. 3 and 6 lead to the same results for the width and position of the maximum of the DF as a function of the parameter ν . The ranges $\nu < 1$, $1 < \nu < 4$, and $\nu > 4$ correspond to small, intermediate, and large areas, respectively. The distribution functions for these intervals are given by Eqs. (50), (62), and (65), respectively, in which ν^2 must be replaced by $\nu^{1/2}$.

Our results on the effect of an external agent on the width of the distribution function (in particular, the transition from large to small fluctuations) are also valid for the models in Refs. 1–4, 6. However, the properties of the oscillations in the transparency logarithm when the external agent varies depend on the specific model. In the small-area case ($\nu < 1$), oscillations of amplitude comparable to the width of the distribution function should occur for all models except the one in Ref. 6. The latter model is exceptional because the perforations there are characterized by a single parameter (the number of impurities in a filament); the rate at which the transparency of a filament changes when the external agent varies (i.e., as the transmission coefficient through the impurities changes) therefore depends only on the filament transparency itself, so that it is impossible for the perforations to “overtake” one another.

We observe in closing that although the distribution functions found above for large-area specimens are exponentially narrow, their width is bounded from below in practice. First, the quantity Q_0 cannot be too large if the transmission of the specimen is to be observable; second, ν turns out to be ~ 1 even for very large specimens. As an estimate let us choose $Q_0 = 40$; for a perforation of diameter 100 Å the values $\nu = 1, 1.2$, and $2^{1/2}$ correspond to sample dimensions 0.2, 1.6, and 140 mm, respectively. The corresponding widths of the DF calculated using (55), (64), and (66) are 0.25, 0.12, and 0.017.

We are grateful to B. I. Shklovskii for helpful discussions, and to A. L. Éfros and Yu. F. Berkovskaya for help with the numerical calculations.

APPENDIX I

We rewrite the definition (14) of the correlation function as

$$K(F_1, F_2) = \lim_{s \rightarrow 0} \int_{-\infty}^{\infty} dQ_1 \int_{-\infty}^{\infty} dQ_2 Q_1 Q_2 (\varphi_{F_1, F_2}(Q_1, Q_2) - f_{F_1}(Q_1) f_{F_2}(Q_2)) \exp[-(se^{-Q_1} + se^{-Q_2})]. \quad (\text{A1.1})$$

Inserting expressions (11) and (9) for ϕ_{F_1, F_2} and f_F and making the change of variable $\sigma = e^{-Q}$, we get

$$K(F_1, F_2) = \lim_{s \rightarrow 0} \frac{1}{(2\pi)^2} \int_0^{\infty} d\sigma_1 \int_0^{\infty} d\sigma_2 \int_{-\infty}^{\infty} dt_1 \int_{-\infty}^{\infty} dt_2 \ln \sigma_1 \ln \sigma_2 \times [\chi_{F_1, F_2}(it_1, it_2) - \chi_{F_1, F_2}(it_1, 0) \chi_{F_1, F_2}(0, it_2)] \times \exp[(it_1 - s)\sigma_1 + (it_2 - s)\sigma_2]. \quad (\text{A1.2})$$

Interchanging the order of integration over t and σ reduces Eq. (A1.2) to

$$K(F_1, F_2) = -\frac{1}{(2\pi)^2} \int dz_1 \int dz_2 [\chi_{F_1, F_2}(z_1, z_2) - \chi_{F_1, F_2}(z_1, 0) \chi_{F_1, F_2}(0, z_2)] \Psi(z_1) \Psi(z_2), \quad (\text{A1.3})$$

where

$$\Psi(z) = \int_0^{\infty} d\sigma \ln \sigma e^{(z-s)\sigma}, \quad (\text{A1.4})$$

and the integration over z_1 and z_2 in (A1.3) is along the imaginary axis (the counter C in Fig. 5). We convert this into an integration over the real axis by deforming C into C' , which passes along the edges of the cut (Fig. 5). The cut is necessary in order for $\Psi(z)$ to be continued analytically into the right-hand halfplane; the continuation is given by

$$\Psi(z) = -\frac{1}{z-s} \int_0^{\infty} dv e^{-v} \ln v - \frac{\ln(s-z)}{s-z}. \quad (\text{A1.5})$$

We note that the expression in the square brackets in (A1.3) vanishes when either z_1 or z_2 is zero. The first term in (A1.5) therefore does not contribute to the integral in (A1.3), because the residues at the poles $z_1 = s$ and $z_2 = s$ tend to zero as $s \rightarrow 0$. Equation (15) follows by substituting (A1.5) into (A1.3) and noting that the values of $\ln(s-z)$ on the top and bottom edges of the cut differ by $-2\pi i$.

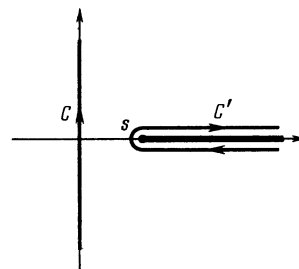


FIG. 5.

APPENDIX 2

In our heuristic derivation of Eq. (18) we will assume that the perforation has the same longitudinal and transverse dimensions, both equal to x_t , and that the fluctuation concentration of the impurities is constant and equal to N throughout the perforation. The probability of formation for such a perforation is e^{-Q} , where

$$\Omega = N^2 x_t^3 / N_D. \quad (\text{A2.1})$$

The tunneling transparency of the barrier near a perforation can be estimated by Eq. (17) with $F = 0$ and $V \sim \varepsilon_g$. Since we are interested in perforations with a given transparency e^{-u} , we obtain the relation

$$u = (m\varepsilon_g)^{1/2} x_t / \hbar. \quad (\text{A2.2})$$

Because the change in the potential over the tunneling length x_t due to the excess charge near the perforation is equal to ε_g , the quantities N and x_t are related by the Poisson equation

$$\varepsilon_g / x_t^2 = e^2 N / \kappa. \quad (\text{A2.3})$$

The desired expression for the concentration $\rho_0(u)$ of perforations coincides to exponential accuracy with the probability e^{-Q} for formation of a perforation with transparency e^{-u} . Using (A2.2) and (A2.3) to express N and x_t in terms of u and substituting the result into (A2.1), we obtain

$$\ln \rho_0(u) = -\Omega = -\frac{1}{u} \left[\left(\frac{\kappa}{e^2} \right)^2 \frac{\varepsilon_g^{3/2} m^{1/2}}{\hbar N_D} \right]. \quad (\text{A2.4})$$

It is easy to see that the expression in the square brackets coincides up to a numerical factor with Q_0^2 , where Q_0 is given by Eq. (19).

APPENDIX 3

We rewrite the distribution function (50) in the form

$$f(Q) = \frac{e^{-\Delta}}{2\pi i} \int_C dz \exp(z e^{-\Delta} - z^{\nu^2}), \quad (\text{A3.1})$$

where the path of integration C in the complex plane is shown in Fig. 6. The integrand in (A3.1) has a saddle point at $z = z_0 = (\nu^2 e^{\Delta})^{1/(1-\nu^2)}$ on the real axis. We shift C so that it passes through the point z_0 (contour C_1 in Fig. 6). For $\Delta \gg 1$ the integral along C_1 can be evaluated by the method of steepest descent, because most of the contribution comes from values z such that $|z - z_0| \ll z_0$. This leads to Eq. (51a).

To derive the asymptotic formula (51b), we deform C into the contour C_2 passing along the edges of the cut in Fig. 6. Expression (A3.1) then becomes

$$f(Q) = \frac{e^{-\Delta}}{\pi} \int_0^{\infty} dt \exp(-t e^{-\Delta} - t^{\nu^2} \cos \pi \nu^2) \sin(t^{\nu^2} \sin \pi \nu^2). \quad (\text{A3.2})$$

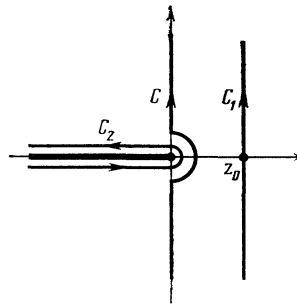


FIG. 6.

For $\Delta < 0$ and $|\Delta| \gg 1$, most of the contribution to the integral comes from values $t \ll 1$. We can therefore replace the sine by its argument and omit the second term in the exponential; the resulting integral is readily evaluated to yield (51b).

Expression (A3.2) is also useful for finding the distribution function when $\nu \ll 1$. In this case it simplifies to

$$f(Q) = \nu^2 e^{-\Delta} \int_0^{\infty} dt t^{\nu^2} \exp(-t e^{-\Delta} - t^{\nu^2}), \quad (\text{A3.3})$$

which after the change of variable $u = t e^{-\Delta}$ gives

$$f(Q) = \nu^2 e^{\Delta \nu^2} \int_0^{\infty} du u^{\nu^2} \exp(-u - u^{\nu^2} e^{\Delta \nu^2}). \quad (\text{A3.4})$$

Since this integral converges for $u \sim 1$, we can replace u^{ν^2} in the integrand by 1 when $\nu \ll 1$, and Eq. (53) follows immediately.

¹¹This quantity is calculated more rigorously in Ref. 10 for the model in Ref. 1. The mesoscopic behavior of the temperature dependence of the transparency logarithm for this model was pointed out in Ref. 11.

¹M. Pollak and J. J. Hauser, Phys. Rev. Lett. **31**, 1304 (1973).

²I. M. Lifshits and V. Ya. Kirpichenkov, Zh. Eksp. Teor. Fiz. **77**, 989 (1979) [Sov. Phys. JETP **50**, 499 (1979)].

³M. V. Krylov and R. A. Suris, Zh. Eksp. Teor. Fiz. **88**, 2204 (1985) [Sov. Phys. JETP **61**, 1303 (1985)].

⁴V. N. Gusyatinikov and R. A. Suris, Fiz. Tekh. Poluprovodn. **18**, 1077 (1984) [Sov. Phys. Semicond. **18**, 670 (1984)].

⁵M. É. Raïkh and I. M. Ruzin, Fiz. Tekh. Poluprovodn. **19**, 1217 (1985) [Sov. Phys. Semicond. **19**, 745 (1985)].

⁶I. M. Lifshits, S. A. Gredeskul, and L. A. Pastur, Zh. Eksp. Teor. Fiz. **83**, 2362 (1982) [Sov. Phys. JETP **56**, 1370 (1982)].

⁷B. L. Al'tshuler and B. Z. Spivak, Pis'ma Zh. Eksp. Teor. Fiz. **42**, 363 (1985) [JETP Lett. **42**, 447 (1985)].

⁸B. L. Al'tshuler and D. E. Khmel'nitskiĭ, Pis'ma Zh. Eksp. Teor. Fiz. **42**, 291 (1985) [JETP Lett. **42**, 359 (1985)].

⁹V. L. Nguen, B. Z. Spivak, and B. I. Shklovskii, Pis'ma Zh. Eksp. Teor. Fiz. **43**, 35 (1986) [JETP Lett. **43**, 44 (1986)].

¹⁰A. V. Tartakovskii, M. V. Fistul', M. É. Raïkh, and I. M. Ruzin, Fiz. Tekh. Poluprovodn. **21**, 828 (1987) [Sov. Phys. Semicond. **21**, (1987)].

¹¹M. É. Raïkh and I. M. Ruzin, Pis'ma Zh. Eksp. Teor. Fiz. **43**, 437 (1986) [JETP Lett. **43**, 562 (1986)].

Translated by A. Mason